



# Estimating the saturated hydraulic conductivity in a spatially variable soil with different permeameters: a stochastic Kozeny–Carman relation

Carlos M. Regalado<sup>a,\*</sup>, Rafael Muñoz-Carpena<sup>b</sup>

<sup>a</sup> *Dep. Suelos y Riegos, Instituto Canario Investigaciones Agrarias (ICIA), Apdo. 60 La Laguna, 38200 Tenerife, Spain*

<sup>b</sup> *TREC-IFAS, Agricultural and Biological Engineering Department, University of Florida, 18905 SW 280 St., Homestead, FL 33031-3314, USA*

Received 6 July 2003; received in revised form 21 November 2003; accepted 15 December 2003

## Abstract

The spatial variability of the saturated hydraulic conductivity ( $K_s$ ) of a greenhouse banana plantation volcanic soil was investigated with three different permeameters: (a) the Philip-Dunne field permeameter, an easy to implement and low cost device; (b) the Guelph field permeameter; (c) the constant head laboratory permeameter.  $K_s$  was measured on a  $14 \times 5$  array of  $2.5 \text{ m} \times 5 \text{ m}$  rectangles at  $0.15 \text{ m}$  depth using the above three methods.  $K_s$  differences obtained with the different permeameters are explained in terms of flow dimensionality and elementary volume explored by the three methods. A sinusoidal spatial variation of  $K_s$  was coincident with the underlying alignment of banana plants on the field. This was explained in terms of soil disturbances, such as soil compaction, originated by management practices and tillage. Soil salinity showed some coincidence in space with the hydraulic conductivity, because of the irrigation system distribution, but a causal relationship between the two is however difficult to support. To discard the possibility of an artefact, the original 70 point mesh was doubled by intercalation of a second  $14 \times 5$  grid, such that the laboratory  $K_s$  was finally determined on a 140 points  $2.5 \text{ m} \times 2.5 \text{ m}$  square grid. Far from diluting such anisotropy this was further strengthened after inclusion of the new 70 points. The porosity ( $\phi$ ) determined on the same laboratory cores shows a similar sigmoid trend, thus pointing towards a plausible explanation for such variability. A power-law relationship was found between saturated hydraulic conductivity and porosity,  $K_s \propto \phi^n$  ( $r^2 = 0.38$ ), as stated by the Kozeny–Carman relation. A statistical reformulation of the Kozeny–Carman relation is proposed that both improved its predictability potential and allows comparisons between different representative volumes, or  $K_s$  data sets with different origin. Although the two-field methods: Guelph and Philip-Dunne, also follow a similar alignment trend, this is not so evident, suggesting that additional factors affect  $K_s$  measured in the field. Finally, geostatistical techniques such as cross correlograms estimation are used to further investigate this spatial dependence.

© 2004 Elsevier B.V. All rights reserved.

**Keywords:** Saturated hydraulic conductivity; Philip-Dunne permeameter; Canary Islands; Modified Kozeny–Carman; Banana plant; Stochastic model

## 1. Introduction

The spatial dependence of the saturated hydraulic conductivity ( $K_s$ ) has been often investigated (Cressie, 1993; Bosch and West, 1998; Moustafa, 2000).

\* Corresponding author. Tel.: +34-922-476343; fax: +34-922-476303.

E-mail addresses: [cregalad@icia.es](mailto:cregalad@icia.es) (C.M. Regalado), [carpena@mail.ifas.ufl.edu](mailto:carpena@mail.ifas.ufl.edu) (R. Muñoz-Carpena).

Geostatistical tools have been used with this purpose (Cressie, 1993), and have helped researchers in the study of the large variability that  $K_s$  often exhibits in soils (Warrick and Nielsen, 1980; Jury et al., 1991). Additionally, and since the hydraulic conductivity is necessary for predictive hydrological models (Vachaud et al., 1988; Braud et al., 1995; Moustafa, 2000), its spatial distribution is often required. However the direct determination of  $K_s$  requires much effort and is time consuming, because many measurements are required to represent the intrinsic variation. Thus indirect methods, based on other more easily measurable soil properties (such as porosity or texture), are sometimes preferred (Ahuja et al., 1989). With this purpose in mind either empirically or physically based relationships have been developed to predict  $K_s$ . Among these there is the Kozeny–Carman equation (Carman, 1937), a power-law that relates  $K_s$  to porosity ( $\phi$ ):

$$K_s = A\phi^n \quad (1)$$

where  $A$  is a proportionality constant and  $n$  is a fitting parameter. In an attempt to improve the predictions of the above model, some modifications of Eq. (1) have been proposed which replace  $\phi$  with the effective porosity,  $\phi_e$ , calculated as the saturated water content minus the water content at 33 kPa matric potential (Ahuja et al., 1984, 1989). Other investigators have used parameters of the Brooks–Corey or fractal models to replace the exponent  $n$  or the proportionality constant,  $A$  in Eq. (1) by measured water retention parameters (Rawls et al., 1993, 1998; Timlin et al., 1999). Additionally, relation may also include the specific surface area,  $S_e$  ( $\text{m}^2 \text{m}^{-3}$ ), such that (Petersen et al., 1996):

$$K_s \propto \phi^n S_e^{-2} \quad (2)$$

However, the above indirect methods do not always lead to reliable results (Kutilek and Nielsen, 1994), thus researchers have resorted to direct measurements of  $K_s$ . Several laboratory (Klute and Dirksen, 1986) and field direct methods (Amoozegar and Warrick, 1986; Ankeny, 1992; Elrick and Reynolds, 1992) have been proposed to measure this soil hydraulic property. Laboratory methods are based on a simple application of Darcy's law in one dimension. In some cases, these have the disadvantage of introducing artefacts because of soil disturbance (e.g. compaction) and also that the

soil is inhibited from other dominant hydraulic effects present in the field (capillary effects, other dimensional components, etc.). An example of this method is the constant head laboratory permeameter (LP) (Klute and Dirksen, 1986), selected for this work. By contrast, field methods deal with the soil in natural conditions and therefore small scale heterogeneities (structure, texture, flora, fauna, soil composition, etc.) may contribute to the above one-dimensional flow. It is thus expected that these field effects will affect the value and spatial distribution of  $K_s$ , but to what extent this is the case is not well understood. The Guelph (GP) (Reynolds et al., 1983) and Philip–Dunne (PD) (Philip, 1993; Gómez et al., 2001; Muñoz-Carpena et al., 2002) permeameters will be selected in this work as field methods.

Comparison of the estimations of the hydraulic conductivity with different methods on a spatial basis has been poorly investigated in the past (Reynolds and Zebchuk, 1996), and particularly in relation to the effect of agricultural practices on the  $K_s$  distribution. Comparisons of laboratory and field  $K_s$  methods in terms of spatial variability are also rare. In addition studies on the spatial variability of the hydraulic properties of highly micro-aggregated soils, as those of volcanic origin, are scarce (Romano, 1993; Ciollaro and Romano, 1995; Zhuang et al., 2000). The intention of this paper is thus two-fold. Firstly the spatial distribution of  $K_s$  in a drip-irrigated volcanic soil banana plantation in the Canary Islands, is compared using the above three permeameters. In particular we shall concentrate on the performance of the PD in predicting the  $K_s$  spatial variability (since this is an easy to implement and low cost but poorly studied permeameter). Secondly, the predictive capability under field conditions of the Kozeny–Carman relation, which usually makes use of laboratory determinations is investigated. Modified versions of (1) are also investigated, in order to improve its predictability potential and allow for comparison between the different permeameters. By comparing such a relation with the laboratory and field permeameter  $K_s$ , conclusions are drawn about what soil properties may be determining the spatial structure of the saturated hydraulic conductivity in the field. Conclusions are also drawn about the consequences of soil tillage and management practices on the spatial distribution of the soil hydraulic properties of a banana plantation.

## 2. Materials and methods

### 2.1. Soil physical–chemical properties

Vertical undisturbed soil cores were collected at 0.15 m soil depth (top of the core) in stainless steel rings using a centred hammer driven sampler. The core dimensions were 0.056 m internal diameter and 0.04 m high. Water contents in the laboratory for porosity estimation were determined gravimetrically. Field water contents for the PD measurements (see below) were obtained with a Trase Time Domain Reflectometry (TDR) equipment (Soilmoisture Equipment Corp.) using a 0.06 m long three guide probe. A TDR soil specific calibration was carried out since this soil diverges significantly from Topp's equation (Regalado et al., 2003).

Water retention curves (WRC) were determined by means of Tempe cells on 10 steps of pressure up to 90 kPa suction ( $\psi$ ) and Richards pressure plates for these additional pressure steps: 100, 500 and 1500 kPa. For the description of the retention characteristic, the model of Brooks and Corey (1964) was used:

$$\Theta = \frac{\theta - \theta_r}{\theta_s - \theta_r} = \begin{cases} \left(\frac{\psi}{\psi_a}\right)^{-\lambda} & \text{for } \psi > \psi_a \\ 1 & \text{for } \psi \leq \psi_a \end{cases} \quad (3)$$

where  $\lambda$  is the pore-size distribution index—a parameter related to the width of the pore-size distribution;  $\theta$ ,  $\theta_s$  and  $\theta_r$  are the volumetric, saturated and residual water contents, respectively.  $\Theta$  is known as the effective saturation;  $\psi_a$  (L) is the matric potential at the air entry point. Model (3) was fit to the water retention data with the help of the SHYFIT program (Durner, 1995).

For the determination of the specific surface,  $S_e$ , the soil was first sieved to 2 mm, dried in vacuum to constant weight with di-phosphorus pentoxide and finally saturated by adsorption in a sulphuric acid atmosphere (Newman, 1983). We chose this method instead of others more widely used, such as the ethyleneglycol method, because it is well known that the latter overestimates the specific surface in these soils (Fernandez-Caldas et al., 1982; Gonzales-Batista et al., 1982).

Na-Amberlite IR-120 (500  $\mu\text{m}$  mesh) cation exchange resins were used as dispersing agent for soil

texture determination (Bartoli et al., 1991) in air-dried samples. Particle-size distribution was determined by the Bouyoucos densimeter method (Gee and Bauder, 1986).

Clay mineralogy was determined by X-ray diffraction in randomly oriented specimens and oriented samples with glycerol and heat treatments (Philips PW 1720) (Whittig and Allardice, 1986).

### 2.2. Field experimental work

A 850 m<sup>2</sup> (33.3 m  $\times$  25.5 m) greenhouse drip-irrigated banana plantation was selected for sampling and measuring. This was selected because it is representative of the agricultural practices carried out in the Canary Islands on exportation crops (mainly bananas and tomatoes). The plot is terraced with an average soil effective depth of 0.85 m over basaltic fractured rock. The soil has volcanic origin, clay loam texture (36  $\pm$  6% clay, 21  $\pm$  2% silt, 43  $\pm$  7% sand) and exhibits andic properties (bulk density < 0.9 g cm<sup>-3</sup>, Al<sub>0</sub> + 1/2 Fe<sub>0</sub> > 2%, phosphate retention > 85%). The soil may be classified as an Andisol (Armas-Espinel et al., 2003). The andic character translates into a stable micro-aggregation and unusual values of soil bulk density (0.87  $\pm$  0.08 g cm<sup>-3</sup>), porosity (66.42  $\pm$  2.42%) and specific surface area (200  $\pm$  17 m<sup>2</sup> g<sup>-1</sup>). A rectangular regular grid (2.5 m  $\times$  5 m) was laid out on the plot surface yielding 70 grid intersection points (Fig. 1). A regular grid was chosen since this represents a more efficient sampling scheme (Webster and Oliver, 1990). The  $K_s$  measurement and sampling protocol is described elsewhere (Muñoz-Carpena et al., 2002).

### 2.3. Laboratory and field permeameters

Laboratory measurements of  $K_s$  were made on a recirculating constant head permeameter on undisturbed soil cores saturated with calcium sulphate following the procedure described by Klute and Dirksen (1986).

The Guelph permeameter is a constant head well permeameter (Reynolds et al., 1983, 1985) consisting on a mariotte bottle that maintains a constant water level inside a hole augered in the soil. The simultaneous approach for solving the Richard's

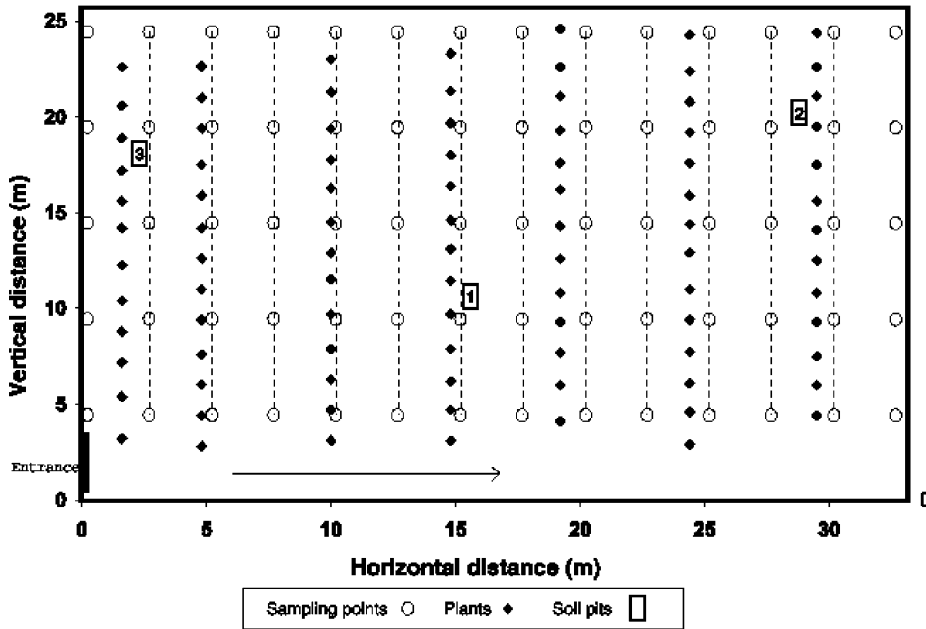


Fig. 1. Sampling points and plant distribution of the experimental plot.

based steady-state equation (Philip, 1985; Elrick and Reynolds, 1992)

$$2\pi H_i^2 K_s + C_i \pi \alpha^2 K_s + 2\pi H_i \phi_m = C_i Q_i \quad (4)$$

requires at least two different water heads in the same well. In Eq. (4)  $\phi_m$  ( $\text{m}^2 \text{s}^{-1}$ ) is the matric flux potential,  $Q_i$  ( $\text{m}^3 \text{s}^{-1}$ ) the steady-state flow rate into the soil, when the steady depth of water in the well is  $H_i$  (m),  $a$  (m) the well radius, and  $C_i$  is a dimensionless proportionality constant dependent on  $H_i/a$ . The augered wells used in this study were 0.06 m in diameter, with 0.05 and 0.1 m constant water levels ( $H_i$ ), and  $C_1 = 0.8$ ,  $C_2 = 1.2$  (double-head method). The double-head method may yield negative  $K_s$  values due to non-attainment of the steady-state, experimental error, soil profile discontinuity (Elrick et al., 1989; Elrick and Reynolds, 1992) and ill-conditioning of the simultaneous equations in  $K_s$  and  $\alpha^* = K_s/\phi_m$  (Philip, 1985). To get around negative  $K_s$  values, a single-head procedure has been proposed, whereby a site estimated  $\alpha^*$  is introduced to avoid the need of a second ponded head (Elrick et al., 1989). The parameter  $\alpha^*$  may be either obtained from soil textural characteristics, from the mean  $\alpha^*$  values of all positive  $K_s$  values or by an optimisation procedure (Mertens

et al., 2002). Alternatively, Vieira et al. (1988), have proposed to recompute the anomalous  $K_s$  values (i.e.  $\phi_m < 0$ ,  $\alpha^* < 1 \text{ m}^{-1}$ ,  $\alpha^* > 100 \text{ m}^{-1}$ ) arising from the double-head method, making use of the conductivity values obtained from the Laplace solution,  $K_L$  (which neglects the capillarity forces in the soil) and the “correct”  $K_s$  values,  $K_s^*$ , via the empirical relation  $K_s^* = \beta K_L^\gamma$ . The fitting parameters  $\beta$  and  $\gamma$  are obtained from the log–log plot of  $K_s^*$  versus  $K_L$ .

The Philip-Dunne permeameter consists of a tube of internal radius  $r_i = 0.018$  m, vertically inserted to a certain depth into a soil borehole with zero gap, and then filled with water up to a height  $h_0 = 0.30$  m at time  $t = 0$ . During infiltration, the times when the pipe is half full ( $t_{\text{med}}$  at  $h = h_0/2$ ) and empty ( $t_{\text{max}}$  at  $h = 0$ ) are recorded, along with soil moisture at the beginning ( $\theta_0$ ) and at the end of the test ( $\theta_1$ ). To obtain the value of  $K_s$  with the PD, the Philip (1993) analysis makes use of a simplification whereby the disk-shaped water supply surface is replaced by a spherical water front of equal area, i.e. of radius  $r_0 = r_i/2$ . If  $R = R(t)$  is the soil wetted bulb radius from the water supply at time  $t$ , then the following differential equation holds

$$\frac{\pi^2 R(R - r_0)}{8r_0 K_s} \frac{dR}{dt} = \frac{\psi_f + h_0 + \pi^2/8}{\Delta\theta} - \frac{R^3 - r_0^3}{3r_0^2} \quad (5)$$

subjected to the initial condition  $R(0) = r_0$ , where  $\psi_f (= \alpha^{*-1})$  is the suction at the wetting front and  $\Delta\theta = \theta_1 - \theta_0$ . Eq. (5) may be integrated to give the temporal variations of the wetted radius and water depth (Philip, 1993). Making use of the two-measured times,  $t_{med}$  and  $t_{max}$  and the increment in soil moisture content,  $\Delta\theta$ , the values of  $K_s$  and  $\psi_f$  can be computed (De Haro et al., 1998; Appendix A in Muñoz-Carpena et al., 2002).

#### 2.4. Statistics

Standard statistics was carried out with SYSTAT 10 (SPSS Inc., 2000) and spatial statistics was performed with VARIOWIN 2.21 (Pannatier, 1996).

### 3. Results and discussion

#### 3.1. Statistical results

The saturated hydraulic conductivity was approximately described by a log-normal probability distribution for the three permeameters (Muñoz-Carpena et al., 2002). Probability plots showed surface area, porosity and the  $\alpha^*$  parameter to be also closely log-normally distributed (results not shown). Mean values of  $K_s$  for the different methods are summarised in Table 1. The LP- $K_s$  ( $27.90 \times 10^{-4} \text{ cm s}^{-1}$ ) is

Table 1  
Mean  $K_s$  values ( $\text{cm s}^{-1}$ )  $\pm$  standard deviation (S.D.) for the laboratory, Philip-Dunne and Guelph permeameters, with the two-head, Laplace, Vieira and 0.05, 0.10 m one-head methods

Permeameter	Method	Mean $K_s \pm$ S.D. ( $\times 10^4$ )
Guelph (GP)	Two-head	$12.07 \pm 8.74$
	Laplace	$10.24 \pm 5.04$
	Vieira	$6.72 \pm 2.61$
	One-head (0.10 m)	$7.77 \pm 4.24$
	One-head (0.05 m)	$5.24 \pm 2.86$
	One-head (0.10 m, $\alpha^* = 0.12$ )	$5.94 \pm 3.36$
	One-head (0.10 m, $\alpha^* = 0.36$ )	$8.42 \pm 4.77$
	Laboratory (LP)	Klute and Dirksen (1986)
Philip-Dunne (PD)	De Haro et al. (1998)	$87.30 \pm 4.95$

placed in between the PD and GP. Differences between field and laboratory methods are well known in the literature (see also discussion below). The PD gives the highest values ( $8.73 \times 10^{-3} \text{ cm s}^{-1}$ ) while the Guelph permeameter shows a decreasing trend from the two-head ( $12.07 \times 10^{-4} \text{ cm s}^{-1}$ ), Laplace ( $10.24 \times 10^{-4} \text{ cm s}^{-1}$ ), 0.10 m one-head ( $7.77 \times 10^{-4} \text{ cm s}^{-1}$ ), Vieira ( $6.72 \times 10^{-4} \text{ cm s}^{-1}$ ) and 0.05 m one-head ( $5.24 \times 10^{-4} \text{ cm s}^{-1}$ ) methods. For the one-head method we used the mean  $\alpha^* = 0.22 \text{ cm}^{-1}$  value obtained from the Vieira analysis. This value for  $\alpha^*$  is placed between  $\alpha^* = 0.12 \text{ cm}^{-1}$ , proposed for structured clay loamy soils and unstructured sands, and  $\alpha^* = 0.36 \text{ cm}^{-1}$  for highly structured soils and coarse sands, and it is thus consistent with the expected  $\alpha^*$  deducible from textural soil characteristics (Elrick et al., 1989). The errors involved by choosing either of these two extreme  $\alpha^*$  values are though small (cf. row 4 with 6 and 7 in Table 1).

#### 3.2. Spatial distribution of $K_s$

Fig. 2 depicts the contour plots of the spatial distribution of  $K_s$  obtained with the three permeameters: LP, GP and PD. It can be seen that the LP- $K_s$  follows a spatial trend that resembles the alignment of banana plants (compare with Fig. 1). Field  $K_s$  exhibits a subtler aligned disposition, which is also smoothed out because of edge effects that render some high  $K_s$  values. Many factors may be responsible for these differences. Flow dimensionality and the representative elementary volume are considered here as the two most relevant.

#### 3.3. Flow dimensionality

Flow dimensionality may be a source of difference among permeameters. Horizontal saturated hydraulic conductivity,  $K_{sh}$ , determinations on a subset of 10 cores showed significant differences between  $K_{sh}$  and  $K_s$  (mean  $K_{sh} = 0.02275 \text{ cm s}^{-1}$  and mean  $K_s = 0.00093 \text{ cm s}^{-1}$ ). Laboratory measurements are mainly prevented from other than one-dimensional flow components. Thus the faster horizontal water flow component may counteract high vertical  $K_s$  values in those permeameters that explore the three space dimensions, i.e. field permeameters, and

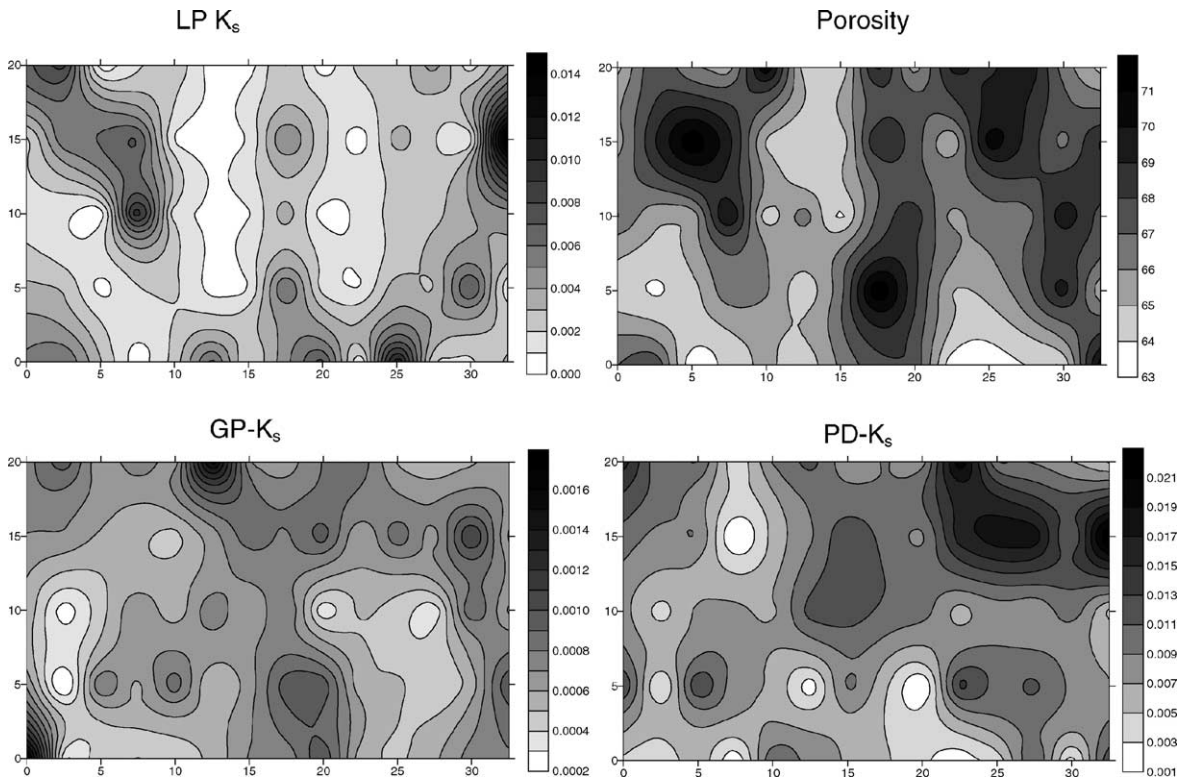


Fig. 2. Contour plots of the spatial distribution of porosity and  $K_s$  as determined by the LP, GP and PD.  $x$ - $y$ -axes labels denote distance (m). The grey scale represents  $K_s$  ( $\text{cm s}^{-1}$ ) or porosity ( $\text{cm}^3 \text{cm}^{-3}$ ) values.

therefore smooth out spatial  $K_s$  differences. Basak (1972) found that the hydraulic conductivity of kaolinite was greater in the horizontal than in the radial direction. X-ray diffraction shows that the dominant mineralogical phases of the studied soil are allophane and halloysite and a minor phase of illite. Halloysite consists of elementary layers of kaolinite and water. Hence the anisotropic orientation of kaolinite may explain the large horizontal conductivity (Basak, 1972), and thus the differences between permeameters. Although the Philip-Dunne permeameter assumes a three-dimensional spherical flow, this is a simplification made for mathematical convenience (see above). The “true” flow is initially one-dimensional and approaches three dimensionality only when  $h_0 - h = 4\Delta\theta_0 r_0$  (Philip, 1993). Such initial disk-shape one-dimensionality may be reinforced because of the orientation of clay particles, and thus yield large PD- $K_s$  values.

### 3.4. Representative elementary volume

The different volume explored by the three permeameters:  $2 \times 10^{-3} \text{ m}^3$  for the PD and  $4 \times 10^{-3} \text{ m}^3$  for the GP versus  $1 \times 10^{-4} \text{ m}^3$  for the LP (Muñoz-Carpena et al., 2002), may be also an important factor that explains  $K_s$  differences, since a larger volume averages over more heterogeneities, and this results in a lower variability in the field methods. This agrees with the values obtained for the coefficient of variability, which is highest for the LP (101%), followed by the PD (56%) and GP (56 and 38% for the single-head and Vieira  $K_s$ , respectively).

### 3.5. Other factors: permeameter assumptions, field heterogeneity, initial water content

Even taking these considerations into account comparison between different methods is difficult because

of underlying assumptions, different response of the permeameter to soil conditions, etc. (Bouma, 1983). Additionally, field specific heterogeneities (flora, fauna, etc.) may also mask  $K_s$  differences within a close neighbourhood. Although soil initial water content,  $\theta_i$ , was not monitored prior to the GP measurements, no correlation was observed between  $\theta_i$  and PD- $K_s$ , contrary to Reynolds and Zebchuk (1996) who found that antecedent water content was slightly correlated with GP- $K_s$ . It is the increment in water content before and after the test has been performed, and not the antecedent water content, what is related to the PD- $K_s$  (see Eq. (5)). Assuming that both PD- $K_s$  and GP- $K_s$  are somehow related, the same would be expected for the Guelph permeameter.

Some low suction values at the wetting front were coincident with large porosities, but with no clear spatial structure (results not shown). This may be due to the large uncertainty implicit in the estimation of  $\alpha^*$  (Mertens et al., 2002).

### 3.6. Banana plants versus $K_s$

Several hypotheses may be explored in order to explain the coincidence of banana plants and LP- $K_s$ . First, the banana root system (exploring the top 0.30 m of the soil) may affect the surrounding soil physical properties. In fact the annual selection of shoots from the mother banana plant yields a spatial “rotation” of plants. This may explain that the matching of plants and LP- $K_s$  is not perfect.

Secondly, localised drip fertigation may modify the hydraulic conductivity of the soil in the neighbourhood of plants. For example Dorel et al. (2000), found that surface desiccation of an Andosol planted with bananas, led to a significant soil shrinkage that affected its hydraulic properties. The accumulation of salts around the wetting bulb may also exert chemical effects upon the soil constituents, which result in alteration of its hydraulic properties (Bresler et al., 1984 and references therein). However, the magnitude of this effect depends not only upon the salt source but also upon the nature of the soil materials. Armas-Espinel et al. (2003) found that low  $K_s$  in volcanic soils was associated with high (Na+Mg)/Ca ratios and low electrical conductivity (EC) values, which they attributed to an increase in swelling pressure. Additionally, excess sodium in low salinity conditions

will decrease hydraulic conductivity through dispersion of fine clay materials. Fig. 3 shows the surface plot of LP- $K_s$ , EC and exchangeable sodium percentage (ESP) of the soil saturation extract. It can be observed an almost exact matching between EC and ESP and certain coincidence of LP- $K_s$  and the salinity status. A cross correlogram analysis (see Section 3.9) shows that EC–ESP correlation is high 0.773 (covariance  $\sigma = 7.96 \times 10^{-2}$ ). According to Emerson (1977), soil swelling pressure raises with increasing ESP and decreasing EC. Therefore a swelling mechanism seems unlikely to explain the spatial distribution of  $K_s$ , since high values of ESP would be counterbalanced by high salinity conditions (Wagenet and Bresler, 1983) (Fig. 3). Salinisation and sodification, induced by irrigation with low quality waters and intensive fertilisation, is frequent in cultivated soils from the Canary Islands—mean CE in this soil is  $4.70 \text{ dS m}^{-1}$ . Also, physical properties of clayey soils can be strongly affected by amorphous materials and oxy-hydroxides of iron and aluminium. Such andic materials induce strong aggregation and impart favourable structural properties such as reduced swelling (El-Swaify, 1975). It is suggested that the spatial coincidence of soil salinity with the hydraulic conductivity, is an artefact of the irrigation system distribution. This is also in agreement with Bresler et al. (1984) who found that soil salinity only accounted for 10–15% of the spatial variability of  $K_s$  in two selected agricultural fields.

Finally field management practices and tillage may introduce soil disturbances, such as soil compaction, and this by turn may affect  $K_s$ . Dorel et al. (2000) showed that soil hydraulic conductivity was drastically reduced in the compacted layers of a mechanised banana plantation, and that soil tillage increased the mean  $K_s$ . Also Moustafa (2000) found that the spatial dependence of  $K_s$  was correlated with the agricultural practices of field soils in Egypt.

### 3.7. $K_s$ versus porosity

From the above discussion it follows that both heterogeneous desiccation and compaction may be responsible for the spatial distribution of  $K_s$ , probably because these affect soil structure. Dorel et al. (2000) showed that the hydraulic effects of both mechanisation and desiccation on an Andosol banana plantation

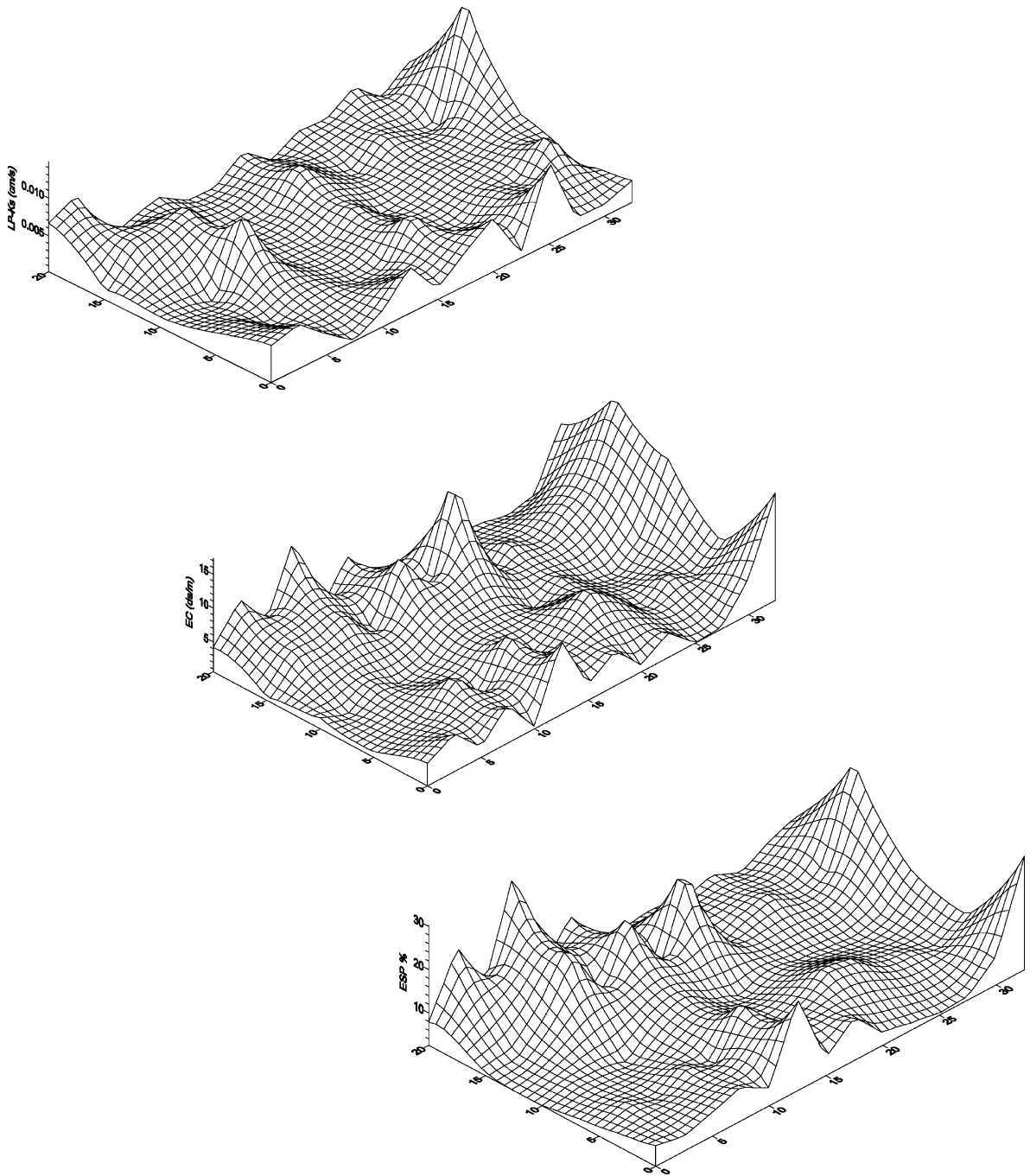


Fig. 3. Surface plots of the laboratory  $K_s$ , electrical conductivity (EC) and exchangeable sodium percentage (ESP) of the soil saturation extract.

were due to changes in soil porosity. The hypothesis of soil compaction would be also consistent with the preferential horizontal orientation of clays in this soil (see above), since compacted clays will be more oriented than non-compacted clays (Al-Tabaa and Wood, 1987). Basak (1972) found that the vertical hydraulic conductivity of kaolinite was more sensitive to the void ratio (volume of voids/volume of solid) than the radial hydraulic conductivity. Thus LP- $K_s$  will be more sensitive to differences in soil compaction than the field methods.

The Kozeny–Carman relation (1) was first tested as a plausible explanatory model for the distribution of  $K_s$ , since also Fig. 2 already points in this direction. Porosity values, obtained on the same cores that LP- $K_s$  were determined, show a power-law relationship of the form:  $K_s = 5 \times 10^{-33} \phi^{16.27}$  ( $r^2 = 0.38$ ) as stated in (1). There exists the possibility that such a correlation between LP- $K_s$  and  $\phi$  may be biased because soil cores were placed inside the lab-permeameter in groups of 10 consecutive samples. In order to discard such an artefact, a second 70 grid point mesh was intercalated in between the first one, such that the laboratory  $K_s$  and porosity were finally determined on a  $2.5 \text{ m} \times 2.5 \text{ m}$  square grid. Additionally, in such a square grid the maximum distance between neighbour sampling points is maximised. Thus unrepresentation and redundancy of some areas is minimised (Webster and Oliver, 1990). The order of introduction of the new soil cores in the LP was randomised to

further discard a possible bias in the  $K_s$  determination. Far from diluting such anisotropy, this was further strengthened, thus suggesting a plausible origin for the spatial distribution of the laboratory conductivity data (Fig. 4).

Comparison of measured and predicted  $K_s$  figures shows that in general predicted  $K_s$  differences have been smoothed out. High LP- $K_s$  values on the left edge have been almost erased and some of the LP- $K_s$  “hot spots” in the plants middle lines have also disappeared. All this indicates that not only porosity but also some other factors may affect the value of  $K_s$ .

In an attempt to look for such factors responsible for the  $K_s$  spatial dependence, we tried a modified Kozeny–Carman relation proposed by Ahuja et al. (1984), where  $\phi$  is replaced by the effective porosity,  $\phi_e$  is calculated as the saturated water content minus the water content at 33 kPa matric potential. Additionally, the relation

$$K_s \propto \phi_e^{3-\lambda} \quad (6)$$

where the exponent  $n$  in (1) has been replaced by the  $\lambda$  parameter of the Brooks–Corey model (3), was also investigated. A linear relation in the log–log space was found between  $K_s$  versus  $\phi_e$  ( $r^2 = 0.36$ ), thus confirming the model of Ahuja et al. (1984). However for model (6) we did not find a simple law of proportionality  $K_s$  versus  $\phi_e^{3-\lambda}$ , but an exponential dependence, although with large data dispersion ( $r^2 = 0.25$ ). This result suggests the possibility of a relation of the form

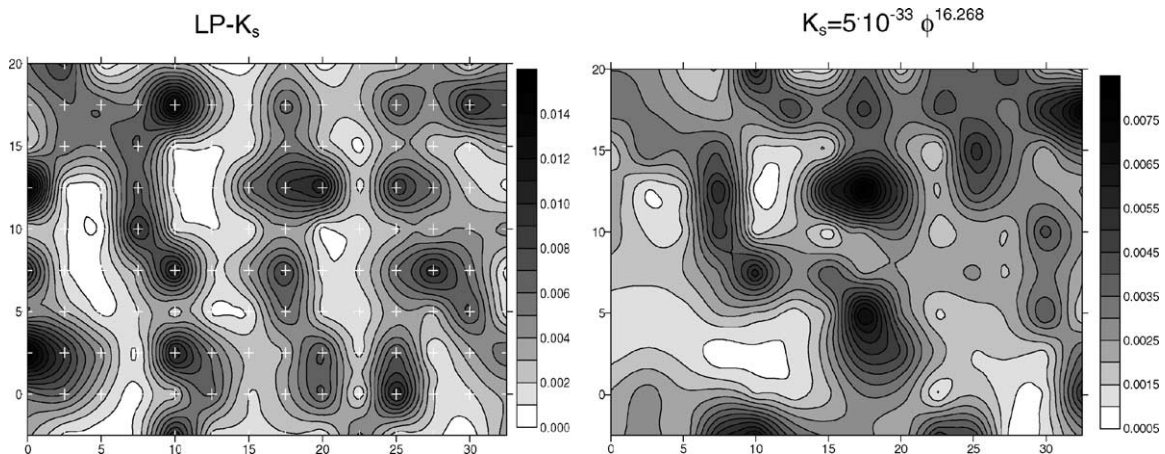


Fig. 4. Contour plots of the spatial distribution of measured vs. estimated LP- $K_s$  as predicted by relation  $K_s = 5 \times 10^{-33} \phi^{16.268}$ . White crosses correspond to sampling points. The grey scale represents  $K_s$  values ( $\text{cm s}^{-1}$ ).  $x$ - $y$ -axes labels denote distance (m).

(Rawls et al., 1993; Timlin et al., 1999)

$$K_s = B(\lambda, \psi_a)\phi^n \quad (7)$$

By plotting  $B$ , calculated as  $K_s/\phi^n$  for fix  $n = 2.5$ , against  $\lambda$  or  $\psi_a$ , we identified a possible functional dependence of this parameter on the air entry potential index. Such dependence is highly non-linear,  $B \propto \exp(\psi_a)$ , although very scattered,  $r^2 = 0.16$  (Regalado and Muñoz-Carpena, 2001). Furthermore, considering the coefficient  $B$  either a function of  $\psi_a$  alone or a combination of  $\lambda$  and  $\psi_a$  in (7), did not significantly improved the predictions of  $K_s$  versus  $\phi_e$ .

### 3.8. A stochastic Kozeny–Carman relation

In this and previous studies (Messing and Jarvis, 1990; Timlin et al., 1999; Zhuang et al., 2000) the fitting results obtained with the Kozeny–Carman equations (1) and (2) are usually poor. In order to improve its predictability potential, the modified versions (6) and (7) have been proposed, although still the scattering is remarkable (Ahuja et al., 1984, 1989). The Kozeny–Carman relation assumes a deterministic point-to-point relationship between  $K_s$  and some soil physical property, such as porosity or surface area. However this hypothesis may not be valid if for example physical properties are determined on samples close to, but from a different location where  $K_s$  has been measured, or if the volume that such properties (e.g. surface area) refer to differs significantly from the representative  $K_s$  volume, and thus averaging  $S_e$  over the whole  $K_s$  volume may not be realistic. This may also explain the lack of accuracy of the above expressions. Hence a statistical reformulation of the Kozeny–Carman equation would be desirable, whereby pairs of observation frequencies replace point-to-point correlations. The following stochastic form of (2) is thus proposed

$$P(K_s) \propto A \cdot \mathfrak{N}(\phi, \mu_1, \sigma_1)^p \mathfrak{N}(S_e, \mu_2, \sigma_2)^q \quad (8)$$

where  $P(K_s)$  is the cumulative frequency of  $K_s$ ;  $\mathfrak{N}(\cdot)$  the normal cumulative distribution function (CDF) of porosity and surface area, respectively, with shape parameters  $\mu_i, \sigma_i$ ;  $A, p, q$  are the fitting parameters. Normal CDFs were first fitted to the cumulative frequencies of  $\phi$  and  $S_e$ . Obtained parameters  $\mu_i$  and  $\sigma_i$  are 0.662, 0.026 ( $r^2 = 0.996$ ) and 172.50, 15.24 ( $r^2 =$

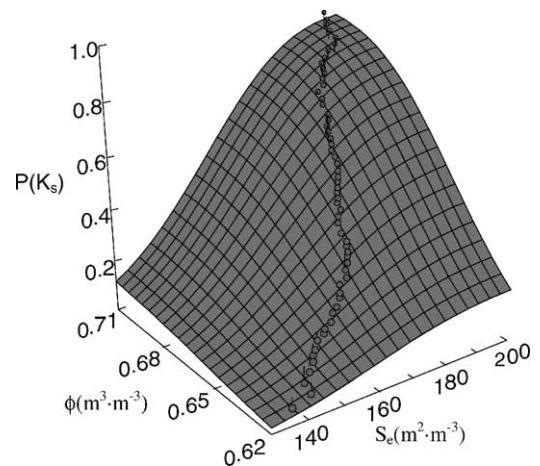


Fig. 5. Agreement between experimental laboratory constant head  $K_s$  data and the proposed stochastic Kozeny–Carman equation (8).

0.998), respectively. These were then substituted into (8) and a least square fitting procedure was used to estimate the parameters  $A = 1.065$ ,  $p = 0.434$  and  $q = 0.552$  from the cumulative frequencies of LP- $K_s$  ( $r^2 = 0.999$ ) (Fig. 5).

The same procedure followed above for the laboratory  $K_s$  data may be pursued with the field determinations. As already discussed, a statistical representation of the Kozeny–Carman equation (1), does not preclude a point-to-point relationship between the fitted variables, and thus the porosity data obtained in the laboratory cores may be used to predict the frequency of Guelph and Philip–Dunne measurements. The following statistical form of (1) was investigated

$$P(K_s) = A \cdot \mathfrak{N}(\phi, \mu, \sigma)^p \quad (9)$$

where  $P(K_s)$  is the cumulative frequency of  $K_s$  and  $A$  is a fitting proportionality constant. Good fit was obtained with the PD data ( $\mu = 0.662$ ,  $\sigma = 0.026$ ,  $A = 0.994$ ,  $p = 0.992$ ,  $r^2$  (observed versus predicted) = 0.987), but a poorer regression (cf. Fig. 6a and b) was achieved with the GP measurements ( $\mu = 0.643$ ,  $\sigma = 0.009$ ,  $A = 0.966$ ,  $p = 0.956$ ,  $r^2$  (observed versus predicted) = 0.966), thus indicating that either the Guelph method is more sensitive to errors in the porosity estimates or it is more affected by other soil properties not considered in (9) (Fig. 6). The values of the constant  $A$  and the power  $p$  in (9) are very close to unity, thus field frequencies may

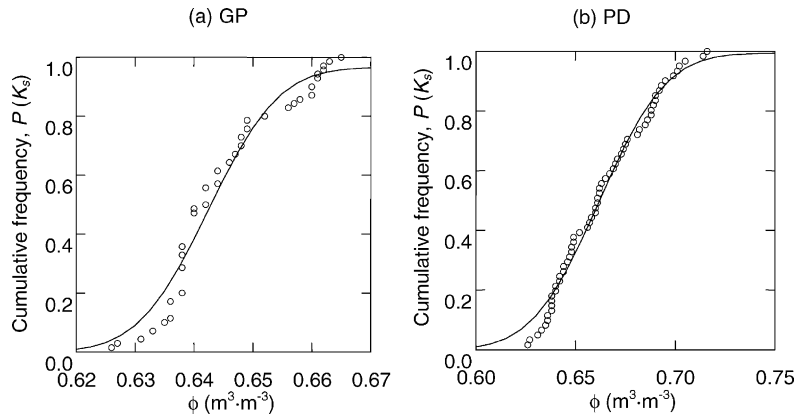


Fig. 6. Agreement between experimental data and the proposed stochastic Kozeny–Carman equation (9) for the field Guelph, GP- $K_s$  (a) and Philip-Dunne, PD- $K_s$  (b) permeameter data sets.

be estimated from porosity values without additional fitting. Furthermore the shape parameters of the PD distribution are the same than the ones obtained for the porosity CDF (see above), indicating that both follow a similar trend of occurrence even though a point-to-point relationship may not be established.

3.9. Geostatistical analysis

Geostatistics is the name proposed for a method of spatial analysis that makes predictions from a sample data, whose relative spatial locations are known. In geostatistics it is required that the expectation of a random measurement made at location  $\mathbf{x}$ , is constant. This hypothesis is known as the stationarity assumption, and it is often overlooked by researchers who proceed directly to applying geostatistical tools. By comparing the median versus the squared inter-quartile range (a measure of the data spreading independent of symmetry) for different data transformations, one may find a suitable symmetrising and variance stabilising transformation (Cressie and Horton, 1987). The log-transformation was found to satisfy both criteria, i.e. (1) it made the data symmetric, and (2) it straightened out the data such that variation is no longer a function of location (Regalado and Muñoz-Carpena, 2001).

In order to quantify spatial correlations between variables, we assessed the correlation between adjacent log-transformed porosity and LP- $K_s$  observations. The plot of the estimated correlation coefficient

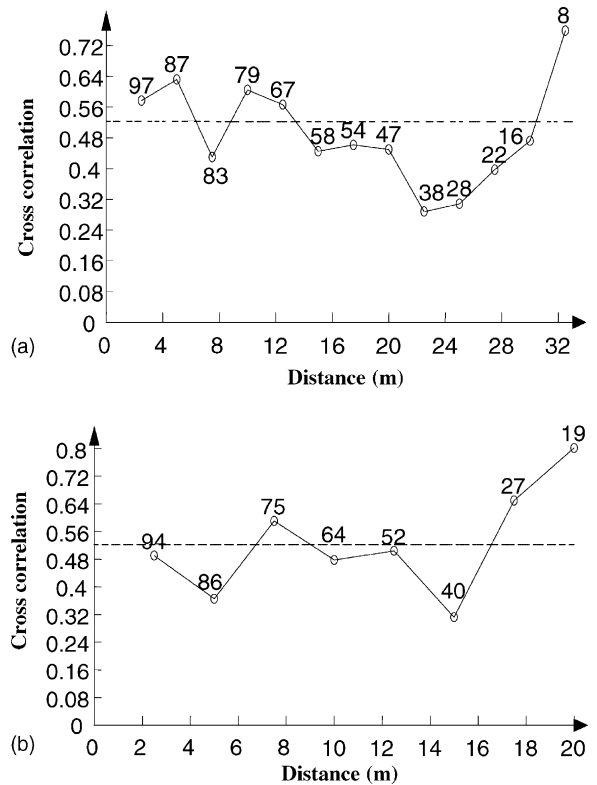


Fig. 7. Directional experimental cross correlograms of log-porosity vs. log-LP- $K_s$ . (a) Horizontal (west-east) direction; (b) vertical (south-north) direction. Numbers on empty circles indicate number of pair comparisons used to compute the correlation coefficient.

of log-porosity versus log-LP- $K_s$  as a function of the separation distance, the so called experimental cross correlogram, is shown in Fig. 7. Directional correlograms in both the horizontal (west-east) direction (Fig. 7a) and vertical (south-north) direction (Fig. 7b) are plotted. It may be observed that although horizontal correlation decreases up to 22.5 m, beyond this an increasing correlation tendency may be observed with the separation distance (an effect previously referred to as the lag effect). The same occurs in the vertical direction for separation distances greater than 15 m. However in general correlation is greater at shorter distances, while large-range correlations are supported by a smaller number of pair comparisons (cf. numbers shown in graph).

#### 4. Summary and conclusions

The saturated hydraulic conductivity is often required for hydrological studies and it is either laboratory or field measured, or it is deduced from other more easily measurable physical soil properties. However, not very often its spatial structure is investigated by comparing different estimation methods. Significant differences observed between  $K_s$  measurements may be partly explained in terms of flow dimensionality and representative elementary volumes, and may be worsened because preferential flow in the horizontal component, originated by orientation of clay particles in this soil. The results shown in this paper indicate that although soil (effective) porosity may be an underlying process determining  $K_s$  distribution, field effects may smooth out this dependence such that this is no longer detectable. We may thus conclude that the spatial variability of  $K_s$  is not an easily distinguishable result of soil porosity or water retention characteristics. This is also affected by other components of the soil (e.g. clay content, degree of aggregation), especially under field conditions, or by the experimental design (e.g. measurement technique). All these factors are difficult to detect if comparisons between different permeameters are not performed or  $K_s$  measurements are restricted to laboratory determinations. This may also limit the field applicability of indirect  $K_s$  estimation methods of the kind of the Kozeny–Carman model, which usually makes use of laboratory determinations, thus neglecting other field factors more relevant to the soil in

natural conditions. A modified Kozeny–Carman equation defined in statistical terms may overcome these limitations, allowing comparisons between different representative volumes or  $K_s$  data sets with different origin. This is also a rather convenient reformulation, amenable for stochastic modelling or Monte-Carlo simulations of the spatial variability of hydraulic properties, whereby locally defined parameter values are replaced by probability distribution functions of parameters (Braud et al., 1995; Vachaud et al., 1988), and thus this deserves further investigation.

Processes promoting soil degradation as surface desiccation and soil compaction, induced by tillage and localised irrigation, may be responsible for the anisotropy of  $K_s$ . Soil salinity showed some coincidence in space with the hydraulic conductivity, because of the irrigation system distribution, but a causal relationship between the two is discarded, since high values of exchangeable sodium are counterbalanced by high salinity conditions and andic materials that impart favourable structural properties, such as reduced swelling. This had not been detected if detailed information about soil mineralogy and chemical properties had not been available, and we had thus arrived to erroneous conclusions about the origin of the spatial distribution of  $K_s$ . Such considerations of both spatial dependence and measuring technique should very much be taken into account in future studies intending to make use of a single (mean) effective value of the saturated hydraulic conductivity.

#### Acknowledgements

This work has been supported by the Florida Agricultural Experiment Station Journal Series No. R-09021, a Project Grant and Postdoctoral Fellowship from the Spanish INIA-National R & D Program (Project SC99-024-C2-1) and the European Union COST Action 622. The authors would like to thank Dr. J. Jawitz from the Soil and Water Department, University of Florida, for his careful reading and revision of the manuscript.

#### References

- Ahuja, L.R., Naney, J.W., Green, R.E., Nielsen, D.R., 1984. Macroporosity to characterize spatial variability of hydraulic

- conductivity and effects of land management. *Soil Sci. Soc. Am. J.* 48, 699–702.
- Ahuja, L.R., Cassel, D.K., Bruce, R.R., Barnes, B.B., 1989. Evaluation of spatial distribution of hydraulic conductivity using effective porosity. *Soil Sci.* 148, 404–411.
- Al-Tabaa, A., Wood, D.M., 1987. Some measurements of the permeability of kaolin. *Géotechnique* 37, 499–503.
- Amoozegar, A., Warrick, A.W., 1986. Hydraulic conductivity of saturated soils: field methods. In: Klute, A. (Ed.), *Methods of Soil Analysis. Part 1. Physical and Mineralogical Methods*, 2nd ed. Agron. Monogr. 9. ASA, Madison, WI, pp. 735–770.
- Ankeny, M.D., 1992. Methods and theory for unconfined infiltration measurements. In: Topp, G.C., Reynolds, W.D., Green, R.E. (Eds.), *Advances in Measurements of Soil Physical Properties: Bringing Theory into Practice*. SSSA Spec. Publ. 30. SSSA, Madison, WI, pp. 123–141.
- Armas-Espinel, S., Hernández-Moreno, J.M., Muñoz-Carpena, R., Regalado, C.M., 2003. Physical properties of “sorriba”-cultivated volcanic soils from Tenerife in relation to andic diagnostic parameters. *Geoderma* 117, 297–311.
- Bartoli, F., Burtin, G., Herbillon, A., 1991. Disaggregation and clay dispersion of Oxisols: Na resin, a recommended methodology. *Geoderma* 49, 301–307.
- Basak, P., 1972. Soil structure and its effects on hydraulic conductivity. *Soil Sci.* 114, 417–422.
- Bosch, D.D., West, L.T., 1998. Hydraulic conductivity variability for two sandy soils. *Soil Sci. Soc. Am. J.* 62, 90–98.
- Bouma, J., 1983. Use of soil survey data to select measurement techniques for hydraulic conductivity. *Agric. Water Manage.* 6, 177–190.
- Braud, I., Dantas-Antonino, A.C., Vauclin, M., 1995. A stochastic approach to studying the influence of the spatial variability of soil hydraulic properties on surface fluxes. *J. Hydrol.* 165, 283–310.
- Bresler, E.G., Dagan, G., Wagenet, R.J., Lauffer, A., 1984. Statistical analysis of salinity and texture effects on spatial variability of soil hydraulic conductivity. *Soil Sci. Soc. Am. J.* 48, 16–25.
- Brooks, R.H., Corey, A.T., 1964. *Hydraulic Properties of Porous Media*. Hydrology Paper 3. Colorado State University, Fort Collins, CO, pp. 1–27.
- Carman, P.C., 1937. Fluid flow through granular beds. *Trans. Inst. Chem. Eng.* 15, 150–166.
- Ciollaro, G., Romano, N., 1995. Spatial variability of the hydraulic properties of a volcanic soil. *Geoderma* 65, 263–282.
- Cressie, N.A.C., 1993. Applications of geostatistics. In: *Statistics for Spatial Data*. Wiley Series in Probability and Mathematical Statistics. Wiley, New York, pp. 211–276.
- Cressie, N.A.C., Horton, R., 1987. A robust-resistant spatial analysis of soil water infiltration. *Water Resour. Res.* 23, 911–917.
- De Haro, J.M., Vanderlinden, K., Gómez, J.A., Giráldez, J.V., 1998. Medida de la conductividad hidráulica saturada. In: González, A., Orihuela, D.L., Romero, E., Garrido, R. (Eds.), *Progresos en la Investigación de la Zona No Saturada*, Collectanea, vol. 11. Universidad de Huelva, Spain, pp. 9–20.
- Dorel, M., Roger-Estrade, J., Manichon, H., Delvaux, B., 2000. Porosity and soil water properties of Caribbean volcanic ash soils. *Soil Use Manage.* 16, 133–140.
- Durner, W., 1995. SHYPPFIT 0.24, User’s Manual. Research Report 95.1. Department of Hydrology, University of Bayreuth, Germany.
- Elrick, D.E., Reynolds, W.D., 1992. Infiltration from constant-head well permeameters and infiltrometers. In: Topp, G.C., Reynolds, W.D., Green, R.E. (Eds.), *Advances in Measurements of Soil Physical Properties: Bringing Theory into Practice*. SSSA Spec. Publ. 30. SSSA, Madison, WI, pp. 1–24.
- Elrick, D.E., Reynolds, W.D., Tan, K.A., 1989. Hydraulic conductivity measurements in the unsaturated zone using improved well analyses. *Ground Water Monit. Rev.* 9, 184–193.
- El-Swaify, S.A., 1975. Changes in the physical properties of soil clays due to precipitated aluminium and iron hydroxides. I. Swelling and aggregate stability after drying. *Soil Sci. Soc. Am. Proc.* 39, 1056–1063.
- Emerson, W.W., 1977. Physical properties and soil structure. In: Russel, J.S., Greacen, E.L. (Eds.), *Soil Factors in Crops Production in a Semiarid Environment*. University of Queensland Press, St. Lucia, Qld, pp. 78–104.
- Fernandez-Caldas, E., Tejedor-Salguero, M.L., Quantin, P., 1982. *Suelos de regiones volcánicas*. Tenerife, Islas Canarias. Colección Viera y Clavijo. IV. Secretariado de publicaciones de la Universidad de La Laguna, CSIC (in Spanish).
- Gee, G.W., Bauder, J.W., 1986. Particle-size analysis. In: Klute, A. (Ed.), *Methods of Soil Analysis. Part 1. Physical and Mineralogical Methods*, 2nd ed. Agronomy 9. ASA/SSSA, Madison, WI, pp. 383–411.
- Gómez, J.A., Giráldez, J.V., Fereres, E., 2001. Analysis of infiltration and runoff in an Olive Orchard under no-till. *Soil Sci. Soc. Am. J.* 65, 291–299.
- Gonzales-Batista, A., Hernández-Moreno, J.M., Fernández-Caldas, E., Herbillón, A.J., 1982. Influence of silica content on the surface charge characteristics of allophanic clays. *Clays Miner.* 30, 103–110.
- Jury, W.A., Gardner, W.R., Gardner, W.H., 1991. *Soil Physics*. Wiley, New York.
- Klute, A., Dirksen, C., 1986. Hydraulic conductivity and diffusivity: laboratory methods. In: Klute, A. (Ed.), *Methods of Soil Analysis. Part 1. Physical and Mineralogical Methods*, 2nd ed. Agron. Monogr. 9. ASA, Madison, WI, pp. 687–734.
- Kutilek, M., Nielsen, D.R., 1994. *Soil Hydrology*. CREMLINGEN-Destedt: CATENA-Verlag, Catena.
- Mertens, J., Jacques, D., Vanderborght, J., Feyen, J., 2002. Characterisation of the field-saturated conductivity on a hillslope: in situ single ring pressure infiltrometer measurements. *J. Hydrol.* 263, 217–229.
- Messing, I., Jarvis, N.J., 1990. Seasonal variation in field-saturated hydraulic conductivity in two swelling clay soils in Sweden. *J. Soil Sci.* 41, 229–237.
- Moustafa, M.M., 2000. A geostatistical approach to optimize the determination of saturated hydraulic conductivity for large-scale subsurface drainage design in Egypt. *Agric. Water Manage.* 42, 291–312.
- Muñoz-Carpena, R., Regalado, C.M., Álvarez-Benedí, J., Bartoli, F., 2002. Field evaluation of the new Philip-Dunne permeameter

- for measuring saturated hydraulic conductivity. *Soil Sci.* 167, 9–24.
- Newman, A.C.D., 1983. The specific surface of soils determined by water sorption. *J. Soil Sci.* 34, 23–32.
- Pannatier, Y., 1996. *VARIOWIN: Software for Spatial Data Analysis in 2D*. Springer-Verlag, New York.
- Petersen, L.W., Moldrup, P., Jacobsen, O.H., Rolston, D.E., 1996. Relations between specific surface area and soil physical and chemical properties. *Soil Sci.* 161, 9–21.
- Philip, J.R., 1985. Approximate analysis of the borehole permeameter in unsaturated soil. *Water Resour. Res.* 21, 1025–1033.
- Philip, J.R., 1993. Approximate analysis of falling-head lined borehole permeameter. *Water Resour. Res.* 29, 3763–3768.
- Rawls, W.J., Brakensiek, D.L., Logsdon, S.D., 1993. Predicting saturated hydraulic conductivity utilizing fractal principles. *Soil. Sci. Soc. Am. J.* 57, 1193–1197.
- Rawls, W.J., Gimenez, D., Grossman, R., 1998. Use of soil texture, bulk density, and slope of the water retention curve to predict saturated hydraulic conductivity. *Trans. ASAE* 41, 983–988.
- Regalado, C.M., Muñoz-Carpena, R., 2001. Field spatial variability of the saturated hydraulic conductivity as measured with three kinds of permeameters. *ASAE Annual International Meeting*, Paper Number 012147, Sacramento, California, USA.
- Regalado, C.M., Muñoz-Carpena, R., Socorro, A.R., Hernández Moreno, J.M., 2003. Time domain reflectometry models as a tool to understand the dielectric response of volcanic soils. *Geoderma* 117, 313–330.
- Reynolds, W.D., Elrick, D.E., Clothier, B.E., 1985. The constant head well permeameter: effect of unsaturated flow. *Soil Sci.* 139, 172–192.
- Reynolds, W.D., Elrick, D.E., Topp, G.C., 1983. A reexamination of the constant head well permeameter method for measuring saturated hydraulic conductivity above the water table. *Soil Sci.* 136, 250–268.
- Reynolds, W.D., Zebchuk, W.D., 1996. Hydraulic conductivity in a clay soil: two measurement techniques and spatial characterization. *Soil Sci. Soc. Am. J.* 60, 1679–1685.
- Romano, N., 1993. Use of an inverse method and geostatistics to estimate soil hydraulic conductivity for spatial variability analysis. *Geoderma* 60, 169–186.
- SYSTAT 10, 2000. <http://www.systat.com/products/Systat/>. SPSS Inc.
- Timlin, D.J., Ahuja, L.R., Pachepsky, Ya., Williams, R.D., Gimenez, D., Rawls, W., 1999. Use of Brooks–Corey parameters to improve estimates of saturated conductivity from effective porosity. *Soil Sci. Soc. Am. J.* 63, 1086–1092.
- Vachaud, G., Vauclin, M., Balabanis, P., 1988. Stochastic approach of soil water flow through the use of scaling factors: measurement and simulation. *Agric. Water Manage.* 13, 249–261.
- Vieira, S.R., Reynolds, W.D., Topp, G.C., 1988. Spatial variability of hydraulic properties in a highly structured clay soil. In: *Proceedings of the Symposium on Validation of Flow and Transport Models for the Unsaturated Zone*, Ruidoso, NM.
- Wagenet, R.J., Bresler, E., 1983. Soil salinity effects on the spatial variability of hydraulic conductivity. *United States-Israel Binational Agricultural Research and Development (BARD) Fund. Final Report Project No. US-21-79*, Bet Dagan, Israel.
- Warrick, A.W., Nielsen, D.R., 1980. Spatial variability of soil physical properties in the field. In: Hillel, D. (Ed.), *Applications of Soil Physics*. Academic Press, New York, pp. 319–344.
- Webster, R., Oliver, M.A., 1990. *Statistical Methods in Soil and Land Resource Survey*. Oxford University Press, New York.
- Whittig, L.D., Allardice, W.R., 1986. X-ray diffraction techniques. In: Klute, A. (Ed.), *Methods of Soil Analysis. Part 1. Physical and Mineralogical Methods*, 2nd ed. *Agron. Monogr.* 9. ASA, Madison, WI, pp. 331–362.
- Zhuang, J., Nakayama, K., Yu, G.R., Miyazaki, T., 2000. Scaling of saturated hydraulic conductivity: a comparison of models. *Soil Sci.* 165, 718–727.